AN INTERFEROMETRIC MEASUREMENT

OF

INDEX OF REFRACTION

Thesis by

Michael Stewart Shumate

In Partial Fulfillment of the Requirements

For the Degree of

Electrical Engineer

California Institute of Technology

Pasadena, California

1964

(Submitted March 13, 1964)

ACKNOWLEDGEMENTS

The author would like to thank Professor Nicholas George for his assistance and guidance in the research presented herein. Special thanks are due Dr. Alan Johnston of the Jet Propulsion Laboratory for his assistance with the experimental apparatus, for furnishing the crystal samples, and for his comments on the manuscript. This work was supported in part by NASA/JPL W.O. 97479.

The author also wishes to thank Mrs. Olive List and Mrs. Ruth Stratton for their help in the preparation of the manuscript.

ABSTRACT

Of the several common methods for measurement of the index of refraction of solid optical materials, only one, the minimum deviation method, can conveniently be used for materials whose refractive index exceeds 1.8. The minimum deviation method requires that a large prism of the optical material be constructed; this is not always possible or feasible for some crystalline optical materials that are of current interest. A method for measurement of index of refraction is presented which requires a thin flat plate of the optical material and is unlimited in the range of refractive index it can cover.

The method uses a two-beam interferometer to determine the optical path length through the flat plate by tipping away from normal incidence through a measured angle. It may be used in the visible portion of the spectrum directly, or extended to other spectral regions with the use of a suitable detector. The technique is shown to have an overall accuracy of $\pm$ 2 x 10^{-4} in the refractive index. An error analysis is presented which shows that sample plates that have a small wedge angle may be used with only slight deterioration in the accuracy. The method is applied to the measurement of the principal indices of refraction of crystalline barium titanate at several wavelengths in the visible spectrum.

An analysis of methods for using an interferometer to determine gradients of refractive index as well as refractive index dispersion is also presented.

TABLE OF CONTENTS

CHAPTER I

INTRODUCTION

The refractive index of an optically transparent material is a dimensionless number which is the ratio of the velocity of light in a reference medium, usually air, to the phase velocity of light in the material itself. In addition to being different for different materials, the refractive index is a function of the wavelength of the electromagnetic radiation illuminating the material and the temperature of the material. It may also vary in the presence of externally applied electric and magnetic fields.

Knowledge of the refractive index of materials is very important and useful in many areas of engineering and physics. For example, refractive index may be used to determine composition for chemical analysis and for process control; it is essential for the design of optical systems involving refracting elements; and it may be used for mineral identification and classification. Refractive index data for almost all known transparent and crystalline materials exist in the common physical handbooks, although it is usually given for only one or a few wavelengths in the visible portion of the electromagnetic spectrum. A variety of instruments for the determination of refractive index are commercially available.

The advent of optical masers has produced the requirement for more precise measurement of the refractive indices of certain crystalline materials which exhibit the phenomenon of second harmonic generation

of light. When an intense beam of single frequency radiation from a laser is allowed to pass through such a crystal, a beam of electromagnetic radiation at the second harmonic frequency is generated (1,2,3). The intensity of the second harmonic beam depends upon many factors including the intensity of the fundamental beam. The usual method of increasing the second harmonic output of a given crystal is to increase the intensity of the fundamental beam. It is possible, however, to attain several orders of magnitude increase in the intensity of the second harmonic beam if the experimental geometry can be preselected so as to have the phase velocity of the fundamental beam be identical with the phase velocity of the induced second harmonic beam (4,5,6). A detailed knowledge of the refractive indices of the particular crystal at the fundamental and second harmonic frequencies is necessary in order to determine if such "velocity matching" is possible.

In this thesis, a method for determination of refractive index is reported which has moderate accuracy. It appears to be particularly well suited for the measurement of refractive indices of crystalline materials. The method was specifically developed to accommodate samples in the form of thin, flat plates since one of the crystalline materials to be investigated is available only in that shape. The method presented is shown to have an ultimate accuracy of $\pm$ 2 x 10^{-4} in refractive index if the test sample is of good optical quality.

The remainder of this chapter is devoted to a description of the common methods of refractive index measurement. Chapter II presents a description and analysis of the particular method selected for the

measurement, along with an error analysis. Chapter III contains the analysis of a method for determination of changes in the refractive index as a function of certain environmental conditions such as temperature, electric field and magnetic field, as well as the analysis of a method for determination of the derivative of the refractive index with respect to wavelength. A description of the apparatus used for the experimental part of this research is presented in Chapter IV.

The method for determination of refractive index was applied to three different materials, and the results are presented in Chapter V. Two of the materials were samples whose refractive index had been previously determined by other methods, and were used as an accuracy check. The third material was crystalline barium titanate, a material that is of current interest as far as its optical harmonic generation properties is concerned (7,8). The principal indices of refraction of barium titanate are currently known at only one wavelength in the visible portion of the spectrum (15). The method of Chapter III for determination of the derivative of the refractive index was applied to barium titanate, and the results are also presented in Chapter V.

1.1 Common Refractive Index Measurement Methods

The measurement of the refractive index of an optically transparent, solid material can be accomplished by any of several methods (9) that can generally be classified into two categories. One type uses the phenomenon of refraction itself under carefully controlled conditions, while the second type uses comparison techniques between the unknown sample and some known reference material.

Controlled Refraction Methods

Three standard methods based upon controlled refraction are summarized below. The choice of a particular method depends upon the accuracy desired and the nature of the sample.

1. Immersion method. The sample, in any irregular shape, is immersed in a mixture of liquids of known refractive indices, and the concentration, and hence the refractive index of the liquid mixture, is changed by addition of more liquid of higher or lower refractive index. When the index of the liquid mixture exactly matches that of the sample, the sample will be invisible in the mixture, due to a complete lack of refraction at the liquid/solid interfaces. The refractive index of the liquid mixture is then measured on an critical angle type refractometer. The method has an accuracy of about $\pm$ 1 x 10^{-3}, and is restricted to indices less than 1.8 because there are no liquids with refractive indices greater than that value.
2. Critical angle method. The sample with one polished face is placed in optical contact with a glass prism whose index is known and is greater than that of the sample. The angle necessary for total internal reflection to occur is then determined, thus allowing calculation of the refractive index of the sample. The method has an accuracy of $\pm$ 1 x 10^{-4} with care, and is restricted to indices less than 1.8 because of the lack of high index reference prism materials.

3. Minimum deviation method. An accurate, large aperture prism of the sample material is constructed, and then placed in an apparatus which measures the deviation angle of a light beam passing through the prism. The angle of incidence between the light beam and the front face of the prism is varied until the minimum deviation angle is determined. Knowledge of the prism angle and the minimum deviation angle allows calculation of the refractive index of the sample. It is possible to attain an accuracy of $\pm 1 \times 10^{-6}$ if the sample prism is large, well constructed and quite homogeneous and the angles are measured to an accuracy of ± 2 seconds of arc. There is no restriction on the maximum determinable index with this method.

Any of the above methods may be adopted for determination of the principal refractive indices of crystals by the use of properly oriented samples and properly oriented polarized light.

Index Comparison Methods

All index comparison methods use a two-beam interferometer as the comparison device (9). The sample in the form of a plane parallel plate is placed in one beam and a suitable reference material, also in the form of a plane parallel plate is placed in the other beam. The difference in the order of interference of the two beams is proportional to the optical path difference and may be used to compute the refractive index of the unknown sample, if the thickness of the two plates and the refractive index of the reference plate are known. The accuracy

of any method based upon this technique is usually not better than $\pm$ 1 x 10^{-4}, due to the limitation imposed by accurate measurement of the thickness of the sample and reference plates. The reference material used is usually air or an evacuated chamber.

An example of such an index-measuring device is the Rayleigh gas interferometer (9,11). Two long gas cells with transparent end plates at each end of each cell are arranged in a division of wavefront type of interferometer. Both cells are usually evacuated, and the interferometer adjusted for zero path difference. The gas whose refractive index is to be determined is then slowly leaked into one cell, and the change in the optical path difference is determined by counting the number of interference orders passed through. The instrument is quite useful for the determination of small index differentials, as between a gas and vacuum or two liquids of similar index. As a differential instrument the accuracy is about $\pm$ 1 x 10^{-6} to $\pm$ 1 x 10^{-7} in index difference. The maximum range of index difference is 5 x 10^{-3} to 5 x 10^{-4}.

Such an interferometer, and for that matter any two-beam interferometer, is not easily used for the direct measurement of the refractive index of liquids and solids with respect to air, since the sample cannot be gradually introduced into the beam of light. It is necessary to resort to some subtle tricks in order to establish the total change of optical path length. A detailed discussion of refractive index determination of solids is presented in Chapter II.

CHAPTER II

USE OF AN INTERFEROMETER FOR REFRACTIVE INDEX DETERMINATION

The measurement of refractive index using a two-beam interferometer may be accomplished simply by placing a sample in one of the beams and determining the change in the order of the interference fringes, given the sample thickness. There exists a serious problem in identifying the interference order as it existed prior to the introduction of the sample, since one monochromatic order looks like the next (11,12). The use of the white light fringes found near equal path lengths is helpful in locating the zero order fringe in monochromatic light, if the optical media through which the white light must travel are not too dispersive and/or are equally the same length in the two beams of the interferometer (11). Then, the change in the order of interference may be determined by the use of a precalibrated rotatable compensator plate located in the other beam of the instrument, or by direct fringe counting. The former principle is used in the Rayleigh interferometer. If, however, the sample is highly dispersive compared to the reference medium, the white light fringes viewed through the sample will be smeared out over many orders, making identification of the zero-order fringe impossible. It is then necessary to resort to an indirect method to determine the total change in the interference order.

Two methods for interferometric index determination are analyzed in detail below. The first method is the direct method, where the shift in interference order is counted directly. The second method

is an indirect method, where the shift in interference order is determined as the result of an incremental measurement (10).

2.1 Analysis of the Methods

In order to mathematically describe these methods a specific type of interferometer, the Twyman-Green version of Michelson's interferometer, will be chosen for the analysis. However, the result of the calculations is valid for any type of two-beam interferometer, provided one is careful to make appropriate changes if the beam traverses the sample in one direction only as in the Jamin and Mach-Zehnder instruments. Furthermore, this analysis assumes air for the reference medium, perfectly collimated incident radiation, and a perfect plane parallel sample. The effects of the lack of these idealizations are treated later in this chapter.

Consider the Twyman-Green interferometer shown in Figure 1. The physical path lengths and refractive indices are noted on each segment of the paths. The optical path lengths for the two beams are:

$$\mathcal{L}_1 = 2\left[n_g \ell_{11} + n_o \ell_{12} + n_s \ell_s + n_o \ell_{13}\right]$$

$$\mathcal{L}_2 = 2\left[n_o \ell_{21} + n_g \ell_{22} + n_o \ell_{23}\right] \qquad (2.1)$$

The order of interference seen in the interferometer is the difference in the path lengths divided by the wavelength of the incident monochromatic radiation.

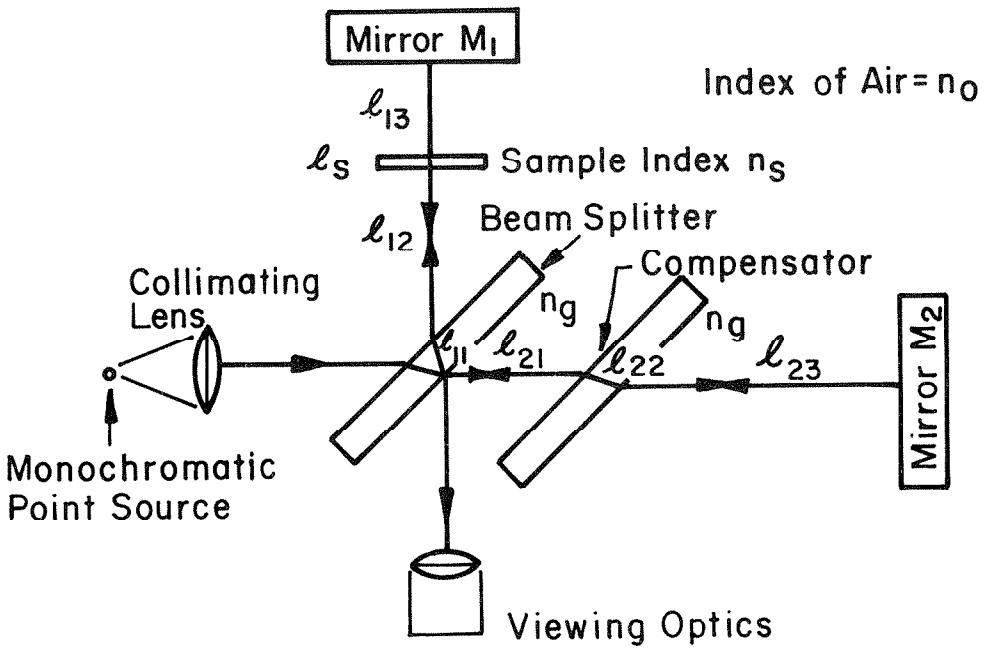

Figure 1: Twyman-Green Interferometer.

$$m = \frac{\mathcal{L}_1 - \mathcal{L}_2}{\lambda_o} = \frac{2}{\lambda_o}\left[n_g(\ell_{11} - \ell_{22}) + n_o\,(\ell_{12} + \ell_{13} - \ell_{21} - \ell_{23}) + n_s\ell_s\right] \qquad (2.2)$$

The interferometer is so constructed that $\ell_{11} = \ell_{22}$. ℓ_{23} can be changed at will in order to locate zero order interference, m = 0.

When the image of mirror M_2 is exactly parallel to mirror M_1, the view field of the interferometer will be uniformly illuminated and have an intensity proportional to $(1 + \cos m\pi)$ for pure monochromatic light. If the image of M_2 is at some slight angle to M_1 several interference orders will be visible across the view field, and are commonly called interference fringes (11). The interferometer is usually adjusted in the latter manner for use as an optical instrument for visual observation.

Method 1. Direct Determination

In this method a direct count is made of the number of fringes which occur between the zero order fringe as viewed through the sample and the zero order fringe with the sample removed. This method can be used only on plane parallel, low dispersion samples; the sample must be plane parallel so that no distortion of the observed fringe pattern occurs (except for a shift in observed position), and the sample dispersion must be low enough so that the zero order fringe may be located.

When ℓ_{23} is adjusted so that the zero order fringe is visible through the sample, $\ell_{23} \triangleq \ell_{231}$, and the interference order fringe viewed through the sample is

$$m = 0 = \frac{2}{\lambda_o} \left[n_s \ell_s + n_o \left(\ell_{12} + \ell_{13} - \ell_{21} - \ell_{231} \right) \right] \qquad (2.3)$$

When the sample is removed and ℓ_{23} is again adjusted so that the zero order fringe is visible through the air path, $\ell_{23} \triangleq \ell_{230}$ and

$$m = 0 = \frac{2}{\lambda_o} \left[n_o \ell_s + n_o \left(\ell_{12} + \ell_{13} - \ell_{21} - \ell_{230} \right) \right] \qquad (2.4)$$

The net change in ℓ_{23} is

$$\Delta \ell = \ell_{231} - \ell_{230} = \frac{n_s - n_o}{n_o} \ell_s$$

The change in the order of interference when ℓ_{23} was changed is counted. Then, using equation 2.2

$$m = \frac{2 n_o \Delta \ell}{\lambda_o} = \frac{2 n_o}{\lambda_o} \left(\frac{n_s - n_o}{n_o} \right) \ell_s$$

Solving for n_s:

$$n_s = n_o + \frac{m \lambda_o}{2 \ell_s} \qquad (2.5)$$

where n_o is usually assumed to be unity. The procedure for refractive index determination using this method is as follows: The interferometer is illuminated with light of the desired wavelength and the zero order fringe is located through the sample. The sample is removed and the number of interference order m that pass when the mirror is moved to

locate the zero order fringe again, is counted. A separate measurement of the sample thickness ℓ_s gives all the data necessary for equation 2.5.

Method 2. Indirect Determination

In this method the optical path length through the sample is determined by an indirect approach which can be visualized with the help of Figure 2. The sample is placed normal to the light beam, tipped through an angle θ and the incremental increase in path length $\Delta\mathcal{L}_s$ noted by counting the change in the order of interference. $\mathcal{L}_s$ can be determined from θ' and $\Delta\mathcal{L}_s$

$$\mathcal{L}_s = \frac{\Delta\mathcal{L}_s \cos\theta'}{1 - \cos\theta'}$$

Since the sample is not completely removed from the interferometer as in the previous method, this method will work for non-plane parallel samples. The following analysis is based on a plane parallel sample; the effect of a non-plane parallel sample will be treated later in this chapter.

To put this on a more formal basis, the change in interference order caused by rotation of the sample through an angle will be derived. Figure 3 shows the sample rotated to an angle θ between two reference planes, with the axis of rotation located at the geometric center of the sample.

From Figure 3 the lengths of the various parts of the path are

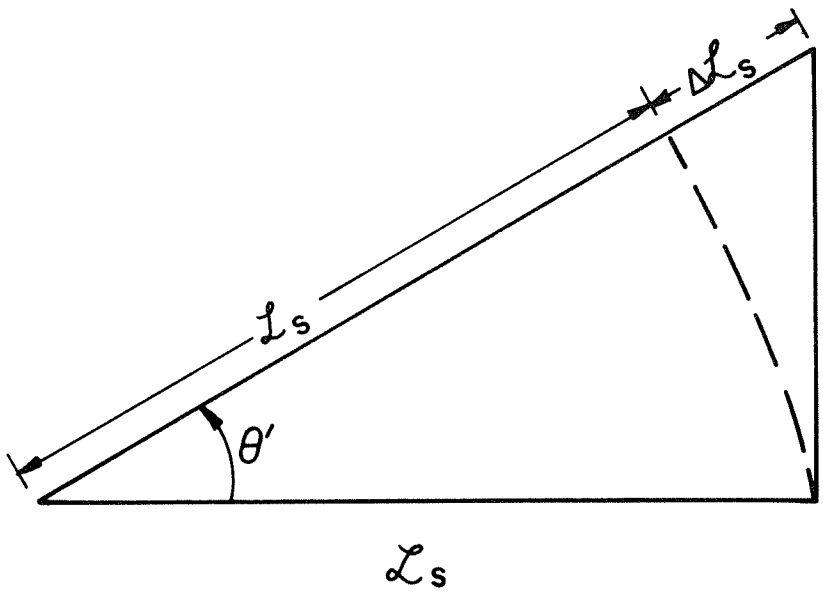

Figure 2: Illustration of the change of the optical path length through a plane parallel sample as a function of angle.

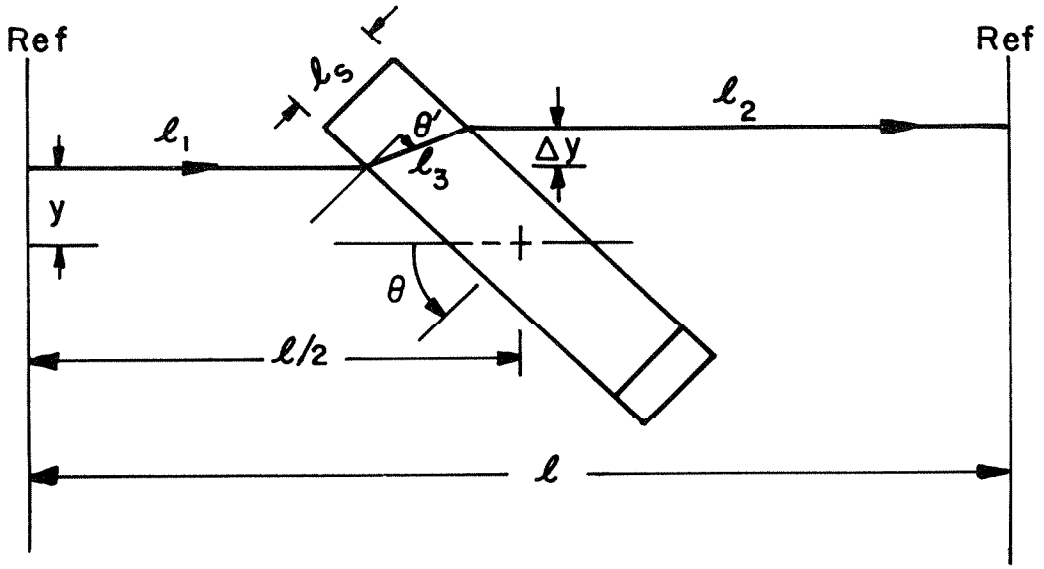

Figure 3: Optical path between two reference planes through rotated sample.

$$\ell_1 = \frac{\ell}{2} - \frac{\ell_s}{2 \cos \theta} - y \tan \theta$$

$$\ell_2 = \frac{\ell}{2} - \frac{\ell_s}{2 \cos \theta} + (y + \Delta y) \tan \theta$$

$$\ell_3 = \frac{\ell_s}{\cos \theta}$$

and

$$\Delta y = \ell_3 \sin (\theta - \theta')$$

The optical path length between the reference planes is

$$\mathcal{L}_t = n_o \ell_1 + n_o \ell_2 + n_s \ell_3 = n_o \ell + \ell_s \left[\frac{n_s}{\cos \theta'} - \frac{n_o}{\cos \theta} + \frac{n_o \sin (\theta - \theta') \sin \theta}{\cos \theta \cos \theta'} \right] \tag{2.6}$$

From Snell's Law

$$\cos \theta' = \frac{\sqrt{n_s^2 - n_o^2 \sin^2 \theta}}{n_s}$$

and

$$\sin (\theta - \theta') = \sin \theta \frac{\sqrt{n_s^2 - n_o^2 \sin^2 \theta}}{n_s} - \frac{n_o}{n_s} \sin \theta \cos \theta.$$

Substituting into equation 2.6 and collecting terms,

$$\mathcal{L}_t = n_o \ell + \ell_s \left[\sqrt{n_s^2 - n_o^2 \sin^2 \theta} - n_o \cos \theta \right] \tag{2.7}$$

The net change in optical path length when the sample is moved from normal incidence to an angle θ is

$$\mathcal{L}_t(\theta) - \mathcal{L}_t(0) = \ell_s \left[\sqrt{n_s^2 - n_o^2 \sin^2 \theta} - n_o \cos \theta - (n_s - n_o) \right] \tag{2.8}$$

Note that this expression is independent of any parameters related to the location of the axis of rotation in the sample. Substituting equation 2.8 into equation 2.2 the net change in the order of interference is

$$m = \frac{2\ell_s}{\lambda_o} \left[\sqrt{n_s^2 - n_o^2 \sin^2 \theta} - n_o \cos \theta - (n_s - n_o) \right] \tag{2.9}$$

Solving equation 2.9 for the sample refractive index:

$$n_s = \frac{\alpha^2 - 2n_o (1 - \cos \theta) \alpha + 2n_o^2 (1 - \cos \theta)}{2 \left[n_o (1 - \cos \theta) - \alpha \right]} \tag{2.10}$$

where

$$\alpha = \frac{m\lambda_o}{2\ell_s}$$

m = change in interference order

λ_o = wavelength of incident radiation

ℓ_s = sample thickness

θ = angle of rotation away from normal incidence

n_o = index of refraction of reference medium

The procedure for index determination using this method is as follows: The interferometer is illuminated with light of the desired wavelength; the sample, mounted on a device for rotating and accurate measurement of the rotation angle, is aligned normal to the beam; the sample is then rotated slowly and the change of the interference order is counted. The maximum angle and/or the size of the order count is determined by the accuracy desired. A separate measurement of the sample thickness, ℓ_s gives all the data necessary for equation 2.10.

These two methods may be used in conjunction with each other, in order to attain improved accuracy. If the test sample is a true plane parallel plate of reasonable thickness, the value of m for Method 1 may be several thousand. m will not in general be an integer however. That is,

$$m = [m] + e \tag{2.11}$$

where $[m] \triangleq$ greatest integer less than m

e = excess fraction of an interference order of m over the integer $[m]$. e is always less than one.

The excess fraction e may be determined directly in the interferometer by viewing the edge of the sample as illustrated in Figure 4. Note that there are two possible choices e and e'. The incorrect one can be eliminated by noting the direction that the fringes move through the view field when the sample is tipped away from normal incidence; e is the correct one if the fringes move down, e' if they move up.

Method 2 is then used to determine which value of [m] should be chosen, and the refractive index may be determined from equation 2.5.

The adaptation of these methods to the measurement of the principal refractive indices of anisotropic crystals is quite simple. When plane polarized light is propagating through an anisotropic medium in such a way that the direction of $\vec{D}$ vector of the wave coincides with one of the principal axes of the crystal, the medium acts like an isotropic one with a refractive index that corresponds to the particular principal axis involved (13). Thus a crystalline sample that is to be used for either the direct or the indirect method must be prepared so that the desired principal axis lies in the plane of the sample, and the sample must be oriented with the direction of that axis parallel to the plane of the $\vec{D}$ vector of the incident polarized radiation. (In the Twyman-Green interferometer of Figure 1 the polarizer may be inserted either between the collimating lens and the beam splitter, or between the beam splitter and the viewing telescope.) In the case of the indirect method, the sample must be oriented with the desired principal

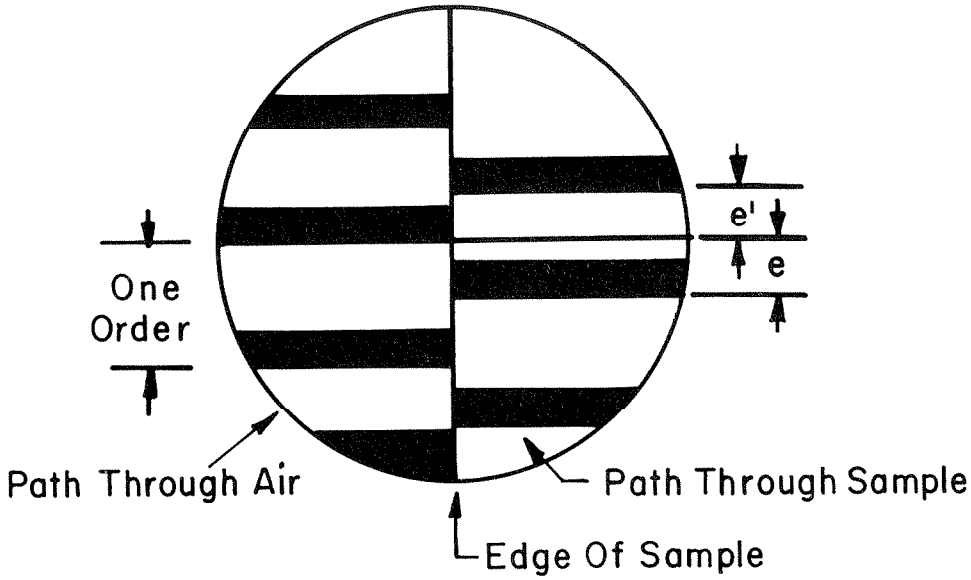

Figure 4: Typical fringe pattern observed when determining the excess fraction of a fringe.

axis parallel to the axis of rotation of the tipping device.

2.2 Analysis of Errors

The primary source of errors in the two methods described above is observational error in the various quantities that must be measured: wavelength of the incident radiation, tip angle, change in the interference order, and sample thickness. There is a secondary source of error in the indirect method if the sample is non-plane parallel. Let us consider the observational errors first.

Of the four observed quantities, the first two, wavelength and angle, can be measured with excellent precision. The sources of radiation used for most interferometric measurements are of the spectral discharge type, and usually have their wavelengths known to five or six significant figures. The angle through which the sample is tipped can be measured with a precision optical coincidence type of angle reading device which has a typical absolute accuracy of ± 2 seconds of arc.

The change in the order of interference is a difficult quantity to measure accurately. In estimations of an arbitrary net change of the interference order by an integral number m plus some fraction e, m is known exactly, but e is usually estimatable to an accuracy of ± 0.1. Some practiced observers have the ability to estimate e to within ± 0.01. Photoelectric fringe counting devices may be constructed to give ± 0.01 accuracy in the interference order (14). If, however, the net change of the interference order is an integral number only, the accuracy of estimation is increased to ± 0.01. Thus in the indirect method if the

tip angle is increased so as to produce only an integral number change in the interference order, the estimation accuracy will be ± 0.01. When the sample is non-plane parallel, there will in general be several interference orders visible across the sample simultaneously. It is thus necessary to determine the change in interference order produced by tipping with respect to some sample fixed reference point. This can usually be accomplished to an accuracy of ± 0.05 in e.

The sample thickness may be measured to an accuracy of ± 0.1 micron by using a conventional gage block comparison technique. However, if the sample is non-plane parallel, there will be a difficulty in measuring the sample thickness at precisely the point used as the fiducial mark for the interference order determination.

The calculation of the resulting errors in refractive index due to the observational errors mentioned above is accomplished by computing the total differential of the expression for refractive index and then substituting typical numbers.

The total differential of equation 2.5 is

$$d\mu_s = \frac{\lambda}{2\ell_s}\, dm + \frac{m}{2\ell_s}\, d\lambda_o - \frac{m\lambda_o}{2\ell_s^2}\, d\ell_s \qquad (2.12)$$

Typical values for the observed quantities and their errors are:

$\lambda_o = 0.5\mu$, $d\lambda_o = 10^{-6}\mu$; $\ell_s = 500\mu$, $d\ell_s = 0.1\mu$; $m = 1000$, $dm = 0.1$.

The following table shows the error that occurs in the measured index

for a specific single measurement error.

TABLE 1

ERROR SUMMARY FOR DIRECT METHOD

Error in n_s	Contributor
0.5×10^{-4}	m accurate to 0.1
0.01×10^{-4}	λ_o accurate to $10^{-6}\mu$ or 0.01Å
1×10^{-4}	ℓ_s accurate to 0.1μ

A similar calculation is performed for the indirect method. The total differential of equation 2.10 is

$$dn_s = \frac{2n_o^2 (1 - \cos\theta)\cos\theta + 2n_o (1 - \cos\theta)\alpha - \alpha^2}{2\left[n_o (1 - \cos\theta) - \alpha\right]^2} \cdot$$

$$\left[\frac{\lambda_o}{2\ell_s}\, dm + \frac{m}{2\ell_s}\, d\lambda_o - \frac{m\lambda_o}{2\ell_s^2}\, d\ell_s\right] - \frac{n_o \alpha \left[2n_o - \alpha\right] \sin\theta}{2\left[n_o (1 - \cos\theta) - \alpha\right]^2}\, d\theta \qquad (2.13)$$

Typical values for the observed quantities and their errors are: $\lambda_o = 0.5\mu$, $d\lambda_o = 10^{-6}\mu$; $\ell_s = 500\mu$, $d\ell_s = 0.1\mu$; $m = 100$, $dm = 0.01$; $\theta = 30^o$, $d\theta = 2$ sec $= 10^{-5}$ rad. A table similar to Table 1 is presented below for the indirect method:

TABLE 2

ERROR SUMMARY FOR INDIRECT METHOD

Error in n_s	Contributor
0.84×10^{-4}	m accurate to 0.01
0.017×10^{-4}	λ_o accurate to $10^{-6}\mu$ or 0.01A^{o}
1.68×10^{-4}	ℓ_s accurate to 0.1μ
0.164×10^{-4}	θ accurate to 2 sec.

Inspection of Tables 1 and 2 reveals that the quantity whose observational error has the largest effect upon n_s is the sample thickness ℓ_s. This effect can be reduced by using a method for sample thickness determination that has higher accuracy than the gage block comparison method. However, such a method usually employs an interferometer and has the disadvantage of being quite tedious and time consuming.

Further inspection of the tables also reveals that the accuracy requirement on the change in interference order m is an order of magnitude higher for the indirect method compared to the direct method. This is due primarily to the larger number of orders counted in the latter method. As mentioned previously on page 18 these two methods may be used in conjunction with each other, with the resulting increase in the accuracy of the interference order assuring that the major source of inaccuracy in the refractive index n_s is due to the uncertainty in the sample thickness.

2.3 The Effects of a Non-Plane Parallel Sample

It is very important to note that in all the discussions up to this point the test sample has been assumed to be perfectly plane parallel; that is, insertion of the sample into the interferometer path results in no change of the light ray directions and at most only a phase delay in the electromagnetic wave. In practice, it is quite difficult to grind and polish a sample so that it is exactly plane parallel. Each face may be easily polished to be flat to within 250Å, but there is usually a slight angle between them, so that the resulting sample acts like a thin prism or wedge, and deviates the light rays slightly. It has been mentioned previously that if the sample is wedge shaped, the direct method for refractive index determination cannot be used, since the fringe pattern becomes distorted when the sample is inserted into the interferometer beam. The indirect method is not affected by the initial distortion of the fringe pattern. However, further distortion in the fringe pattern occurs as the sample is tipped away from normal incidence[1] since the deviation angle of a prism is a function of the angle of incidence. If the indirect method is to be a generally useful laboratory procedure for refractive index determination it should be useful for non-plane parallel as well as plane parallel samples.

The effect of a wedge shape sample is analyzed in the following paragraphs, and is shown to deteriorate the accuracy of the

---

1. Normal incidence for a wedge shaped sample is defined as the ray which intersects the front face of the sample at an angle of 90° to the plane of the front surface.

method by a modest amount.

The exact analysis of the deviation angle of a wedge-shaped sample with a light beam incident at some arbitrary angle is extremely difficult, and would be too detailed for the type of errors involved. The analysis will be restricted to a particular geometry, and will then be generalized to include other cases.

Figure 5 shows the principal plane of a prism in one beam of an interferometer with the axis of rotation of the prism and the apex of the prism both perpendicular to the plane of the figure. With the sample set to normal incidence the mirror is initially adjusted so that the light ray returns on itself. When the sample is rotated through an angle, the ray passes through the sample on the return trip at a different place where the path length is slightly longer. Since the derivation of equation 2.10 assumed the path length to be the same on both passes through the sample, a small error will be introduced.

It can be shown that the change in the deviation angle of a thin prism as a function of the angle of incidence (or angle of rotation) is as follows, where small angle approximations are made wherever appropriate

$$\delta_{||} = n_s \alpha \left[\frac{\sqrt{1 - \frac{\sin^2 \theta}{n_s^2}}}{\cos \theta} - 1 \right] \qquad (2.14)$$

where $\delta_{||}$ = change in prism deviation angle

α = prism wedge angle.

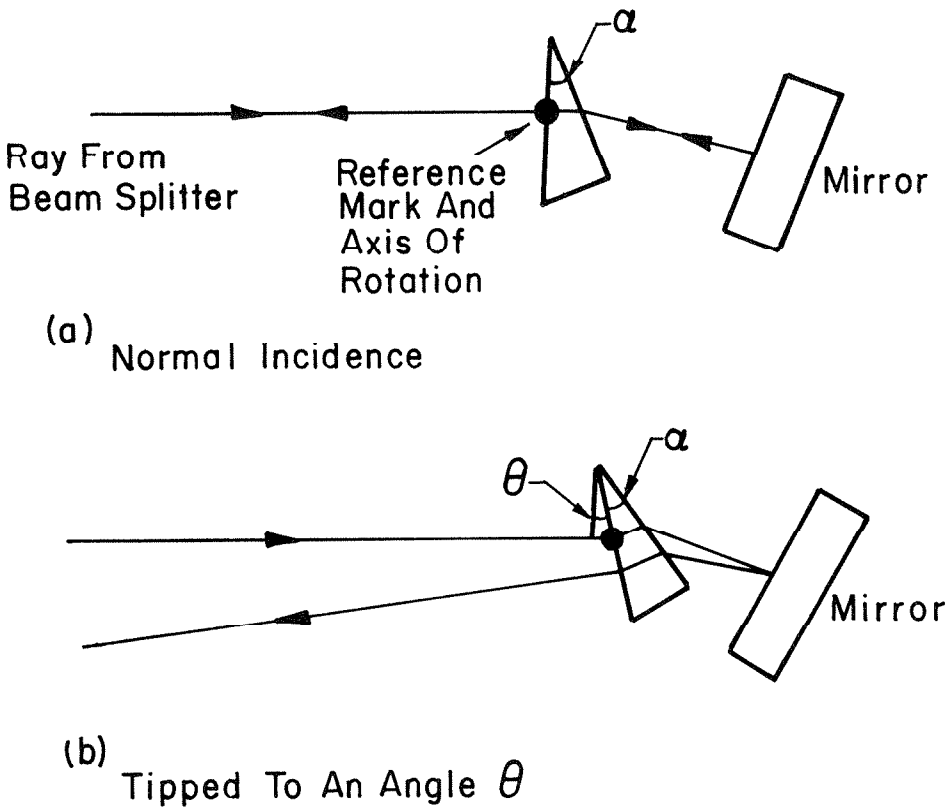

Figure 5: Ray path for a wedge-shaped sample in an interferometer beam.

The incremental change in the physical path length through the sample due to the light ray being deviated through $\delta_{||}$ and reflecting off a mirror d cm. away is

$$\Delta \ell = 4d\, \delta_{||}\, \alpha \tag{2.15}$$

Substituting equation 2.14 into equation 2.15

$$\Delta \ell = 4n_s\, \alpha^2 \left[\frac{\sqrt{1 - \frac{\sin^2 \theta}{n_s^2}}}{\cos \theta} - 1 \right] \tag{2.16}$$

Equation 2.16 represents a θ-dependent correction which must be added to ℓ_s in equation 2.10. Since this is a second order correction, the value of n_s used need be only an approximate one.

The geometrical arrangement that applies for equation 2.14 is that of Figure 5, that is, with the axis of rotation parallel to the apex of the prism. Of course other such geometries are possible and it can be demonstrated that the ideal arrangement is with the apex of the prism perpendicular to the axis of rotation. The change in the prism deviation angle δ is a minimum under this condition. An expression for this angle is derived using the same small angle approximations and the result is presented here:

$$\delta_{\perp} = \alpha \left[\sqrt{n_s^2 - \sin^2 \theta} - n_s + 1 - \cos \theta \right] \tag{2.17}$$

The subscript notation used for the δ's in equations 2.14 and 2.17 denotes the relationship between the axis of rotation and the apex of the prism. The correction to be added to ℓ_s in equation 2.10 is obtained by substituting the appropriate expression for δ into equation 2.15. In order to gain some idea of the magnitude of these corrections, let us substitute some typical numbers:

$n_s = 2.43$, $\alpha = 6'$, $\theta = 30^o$, $d = 5$ cm.

axis parallel to apex: $\ell = 0.193\mu$

axis perpendicular to apex: $\ell = 0.048\mu$

Comparison of these numbers to Table 2 reveals that the accuracy of measurement of n_s deteriorates to approximately 3×10^{-4} in the worst case. The values for d chosen is large, and it is to our advantage to try to arrange the experimental set up so that d is as small as possible.

To summarize, it can be stated that the deteriorating effect of a non-plane parallel sample will be minimized if the sample is placed as close as possible to the mirror with the apex of the wedge perpendicular to the axis of rotation.

A non-plane parallel sample introduces another complication in addition to the one discussed above, which results in errors in estimation of the interference order. The insertion of a non-plane parallel sample into one beam of the interferometer results in interference fringes that are localized in the plane of the mirror (11). Since the sample is usually placed some distance in front of the mirror, it may

not be possible for the viewing optics to be focused on both the sample and the plane of localization simultaneously. The interference order change when the sample is rotated is counted with respect to a sample fixed fiducial mark, and this mark may not be visible when the viewing optics are focused upon the fringes, thus leading to an uncertainty in the ability to count fringes to any reasonable accuracy. This problem may be minimized by placing the sample as close to the mirror as possible.

Another source of influence upon the visibility of the fringes is the lack of perfect collimation of the incident radiation (11). Since it is not possible to have a source of finite brightness with a vanishingly small area, the effective source aperture at the focus of the collimating lens will have a finite diameter, causing the radiation leaving the lens to have a slight divergence angle. A general reduction in the visibility of the fringes results, regardless of the degree of localization. In practice, however, apertures of several millimeter diameter may be used without severe deterioration of the fringe visibility.

CHAPTER III

DETERMINATION OF INDEX GRADIENTS AND INDEX DISPERSION

The refractive index of all optically transparent materials is known to be a function of the wavelength of the electromagnetic radiation used for the refractive index determination. In most cases the variation in index is only a few percent as the wavelength is varied throughout the entire visible portion of the spectrum. The refractive index is also known to be a slowly varying function of one or more environmental factors of the optical material, such as temperature, pressure and externally applied electric or magnetic fields. The same comments apply to the principal indices of refraction of crystalline materials, except that the index variation with temperature may be discontinuous at the Curie temperature.

The two-beam interferometer is very useful for the measurement of these refractive index changes. The material in the form of a plane parallel slab is placed in one beam of the interferometer and is provided with a means of varying the desired parameter, using as a starting place, a point at which the refractive index has been previously measured by any of the methods mentioned in Chapters I and II. The desired parameter is then slowly varied and the change in interference order through the sample is noted simultaneously. A separate determination of the sample thickness allows computation of change of refractive index. The technique is very simple when used for determining index variation with temperature, electric field, etc. but is beset with

a complication when an attempt is made to determine index variation with wavelength of the illumination. Hence, these two situations will be discussed separately.

3.1 Determination of Refractive Index Variation with Temperature, Electric Field, Magnetic Field, etc.

The technique as stated above is quite straightforward (15): the sample, provided with a means of varying the desired parameter, is inserted normal to one of the interferometer beams and the interferometer is illuminated with radiation of the desired wavelength. The movable mirror is adjusted so that the interferometer reference mark is aligned with an integral interference order fringe. The desired parameter is then varied slowly to some new value and the change in interference order is noted. The change in the refractive index may be computed if the sample length is known. Note, however, that the sample length may have varied when the parameter was varied due to thermal expansion, electro- or magneto-striction, etc. These changes must be included in the calculation. The following equation can be used to compute the refractive index at some value of parameter V_2 given the refractive index at V_1.

$$n_s(V_2) = \frac{1}{\ell_s(V_2)} \left[n_s(V_1)\, \ell_s(V_1) + \frac{m\lambda_o}{2} \right] \qquad (3.1)$$

It should be noted that m may be either positive or negative. Care should therefore be exercised in the performance of the experiment to note which direction interference order changed. (That is, it should

be noted whether the optical path length increased or decreased.)

The accuracy requirements are very lax on the observation of the various quantities appearing in equation 3.1 except the initial value of the refractive index. If the interference order change is accurate to 0.1 and the sample thickness is known to 1%, the measured index change will be accurate to one part in the fourth place.

3.2 Determination of Refractive Index Variation with Wavelength of the Illuminating Radiation

The variation of refractive index with wavelength of the illuminating radiation is commonly referred to as dispersion of the refractive index, and can be obtained for a given material by using any of the determination methods mentioned in Chapters I and II at several wavelengths throughout the spectral range desired. This approach is limited by the availability of spectral light sources that have appropriate wavelengths and brightness. A technique is presented here which circumvents this problem by allowing determination of the slope $dn/d\lambda$ at a wavelength where the refractive index has been determined, thus allowing extrapolation of the refractive index to nearby values of wavelength.

The monochromatic light source of the interferometer is replaced with the exit slit of a continuously variable monochromator whose input slit is illuminated with white light. Since the light emanating from the output slit is only quasi-monochromatic, interference fringes will be visible only when the movable mirror is positioned so that m of equation 2.2 is small. This visibility problem prevents direct

determination of a refractive index at some nearby wavelength by a direct fringe count associated with a change in the wavelength of the illumination.

The technique for determining the index slope is as follows. The sample is inserted normal to one of the interferometer beams, the monochromator is set to a wavelength λ_o at which the sample refractive index has already been determined, and the movable mirror is positioned so that as the wavelength drum is moved slightly to either side of λ_o, the fringe pattern remains stationary. This is the condition $dm/d\lambda = 0$ where m is that of equation 2.2.

$$\frac{dm}{d\lambda} = \frac{2\ell_s}{\lambda_o} \frac{dn_s}{d\lambda} - \frac{2}{\lambda_o^2}\left[n_o (\ell_{12} + \ell_{13} - \ell_{21} - \ell_{231}) + n_s (\lambda_o)\, \ell_s\right] \quad (3.2)$$

The sample is now removed from the interferometer and the movable mirror moved to position ℓ_{232} such that $dm/d\lambda$ is again zero. Then,

$$\frac{dm}{d\lambda} = \frac{2}{\lambda_o}\left[n_o (\ell_{12} + \ell_{13} - \ell_{21} - \ell_{232}) + n_o\, \ell_s\right] \quad (3.3)$$

where the first term does not appear as in equation 3.2, since $dn_o/d\lambda = 0$. Substituting equation 3.3 into equation 3.2 and solving, we get

$$\frac{dn_s}{d\lambda} = \frac{1}{\ell_s \lambda_o}\left[n_o (\ell_{232} - \ell_{231}) + (n_s(\lambda_o) - n_o(\lambda_o))\ell_s\right] \quad (3.4)$$

Equation 3.4 gives the slope of the refractive index at λ_o in terms of the distance the movable mirror traveled. It should be noted

that $\frac{dn_s}{d\lambda}$ will for most materials always be negative, so that $(\ell_{232}-\ell_{231})$ will be a negative number. The accuracy of determination of $dn/d\lambda$ is directly dependent upon the method used for determining $(\ell_{232} - \ell_{231})$. The most accurate method would be to illuminate the interferometer with monochromatic light of wavelength λ_o and count fringes. This is quite laborious, since several hundred fringes must be counted, and it is difficult to identify the $dm/d\lambda = 0$ fringe. An easier, but less accurate method is to use a micrometer as a lead screw for the movable mirror, and note the distance by reading the micrometer dial. This leads to a typical accuracy of $\pm 0.016\mu^{-1}$ in the slope of the refractive index.

The refractive index at some other wavelength may be determined to first order by using a Taylor series expansion

$$n_s(\lambda_1) = n_s(\lambda_o) + (\lambda_1 - \lambda_o)\frac{dn_s}{d\lambda} \qquad (3.5)$$

The accuracy of $n_s(\lambda_1)$ will depend upon the interval of extrapolation $\lambda_1 - \lambda_o$, but will in general be accurate to $\pm 2 \times 10^{-4}$ for an interval of $100\,\text{Å}$.

CHAPTER IV

DESCRIPTION OF THE EXPERIMENT

Two methods have been presented in Chapter II for determination of the refractive index of thin, flat transparent plates. Both of these methods depend upon an interferometer as the basic measuring instrument; one method measures the optical path length directly, and the other method indirectly by tipping the sample. Of the two methods the latter has been shown to have more versatility in terms of the type of samples it will accommodate. This method is therefore chosen as the one to be used in the first part of the experimental measurement to be performed.

Chapter III discussed the determination of the variation of refractive index with environmental factors and with wavelength of the illuminating radiation. The interferometric determination of index variation as a function of temperature, electric field, etc. is discussed in the literature (15) and will not be included in the experimental part of this research. The slope of the refractive index is measured in the second part of the experimental measurement.

4.1 Apparatus

The experimental setup is built up around a Michelson interferometer that has been modified with the proper illuminating and viewing optics to convert it into a Twyman-Green interferometer. Furthermore, the interferometer is provided with a mechanism which permits one mirror to be moved in a direction normal to the plane of the mirror, and

a calibrated scale to measure the position of the mirror. A complete diagram of the apparatus is shown in Figure 6, and photographs of the apparatus appear in Figures 7 and 8.

The entire setup was placed upon a shock mounted cast iron surface plate in order to have good isolation from the building vibrations. The unique shock-mount method used is described in Appendix I. The apparatus is also provided with a cover which prevents air currents from disturbing the fringe pattern.

The interferometer is set up with its optics, and the apparatus is provided with a device which is capable of rotating the sample about a horizontal axis and measuring the angle of rotation. This device, a Leitz dividing head, uses a precision optical coincidence technique for measuring the rotation angle of a divided circle that is rigidly attached to the axis of the instrument. The stated accuracy of the instrument is $\pm$ 2 seconds of arc. The dividing head is provided with a sample holder that allows the sample, mounted upon a small brass disc, to be held rigidly in one of the interferometer light beams, with the axis of the dividing head being contained in one of the sample faces. The sample is fastened to the brass disc with wax and is provided with some fine cross wires which serve as a fiducial mark. The brass disc clips into the sample holder, in order to facilitate easy change of the sample. Figure 9 is a photograph of the sample holders and discs.

When the experimental apparatus is set up, three adjustments of importance should be noted. First, the axis of the dividing head

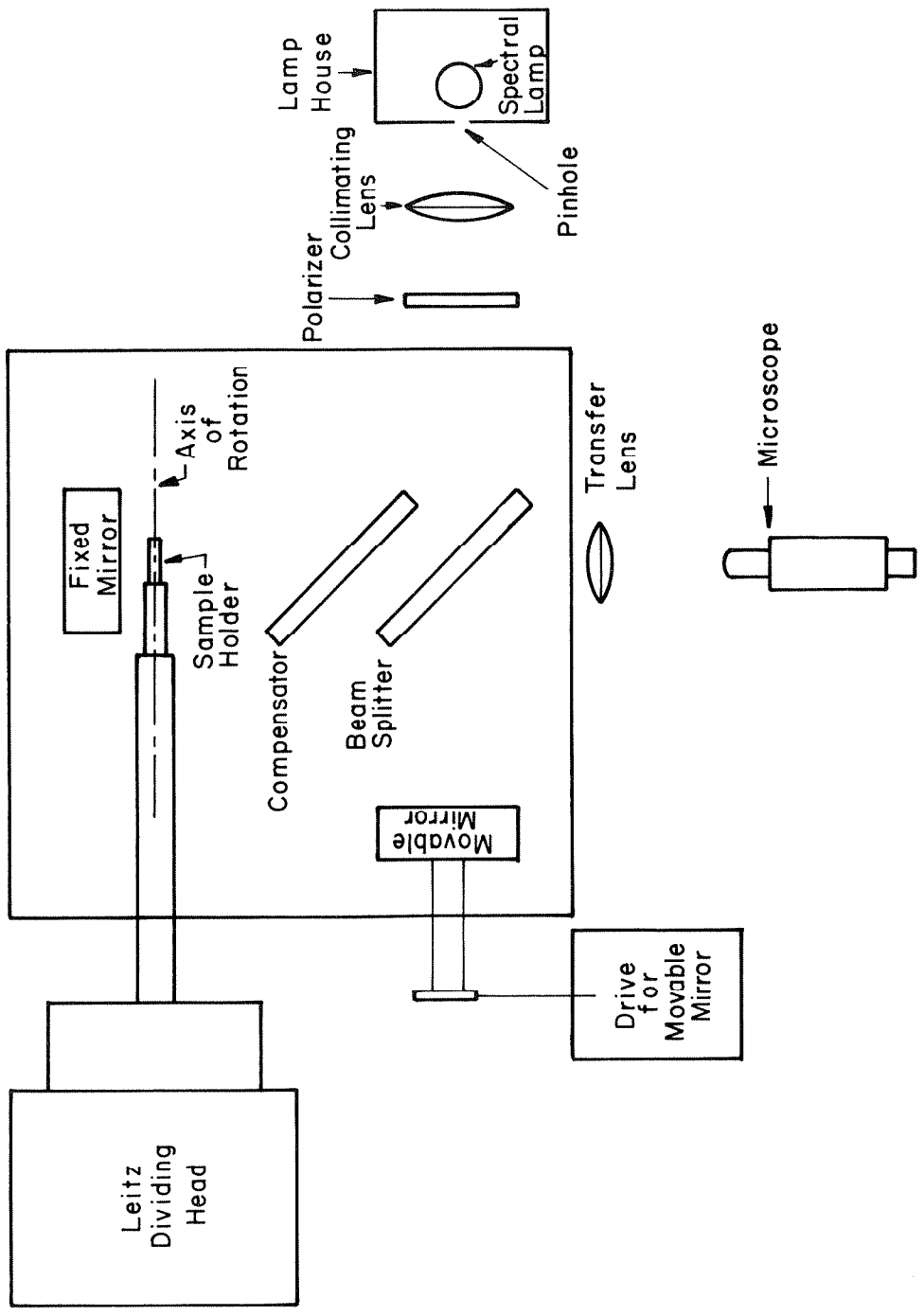

Figure 6: Diagram of experimental apparatus.

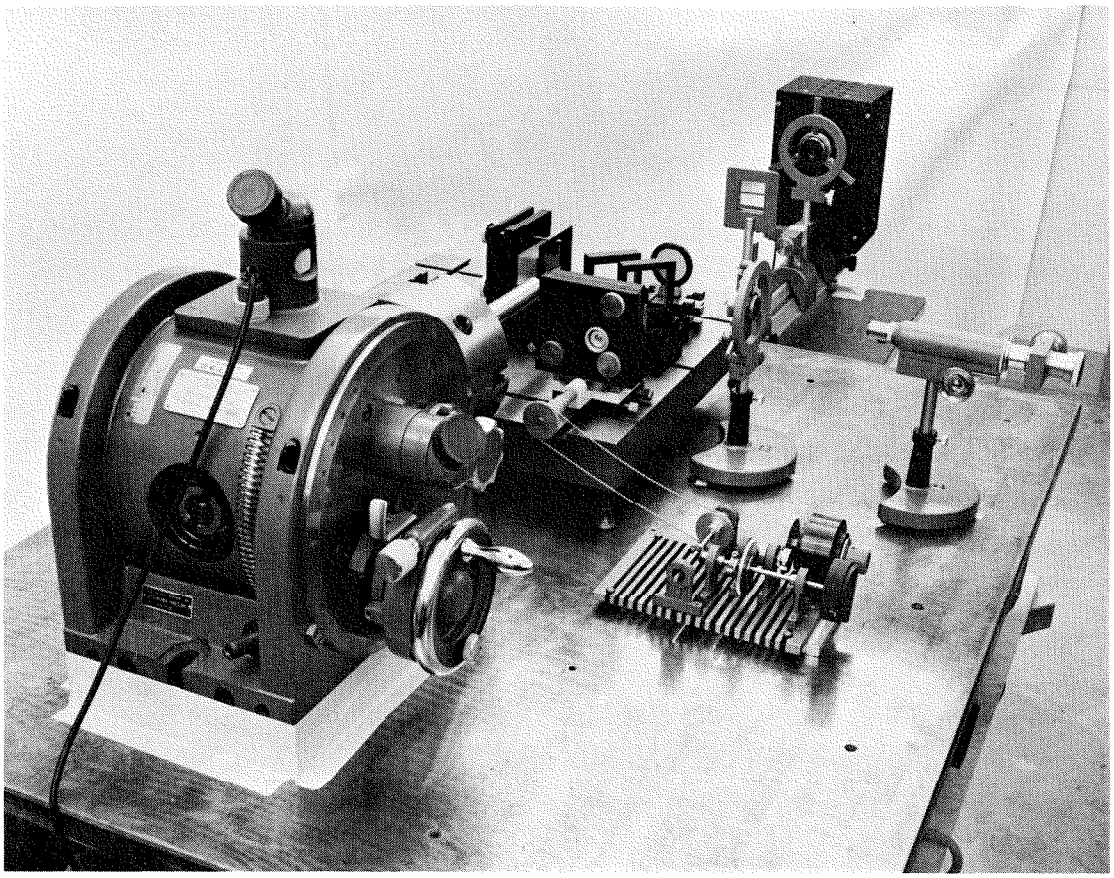

Figure 7: Photograph of the experimental apparatus showing the Leitz dividing head and movable mirror drive mechanism.

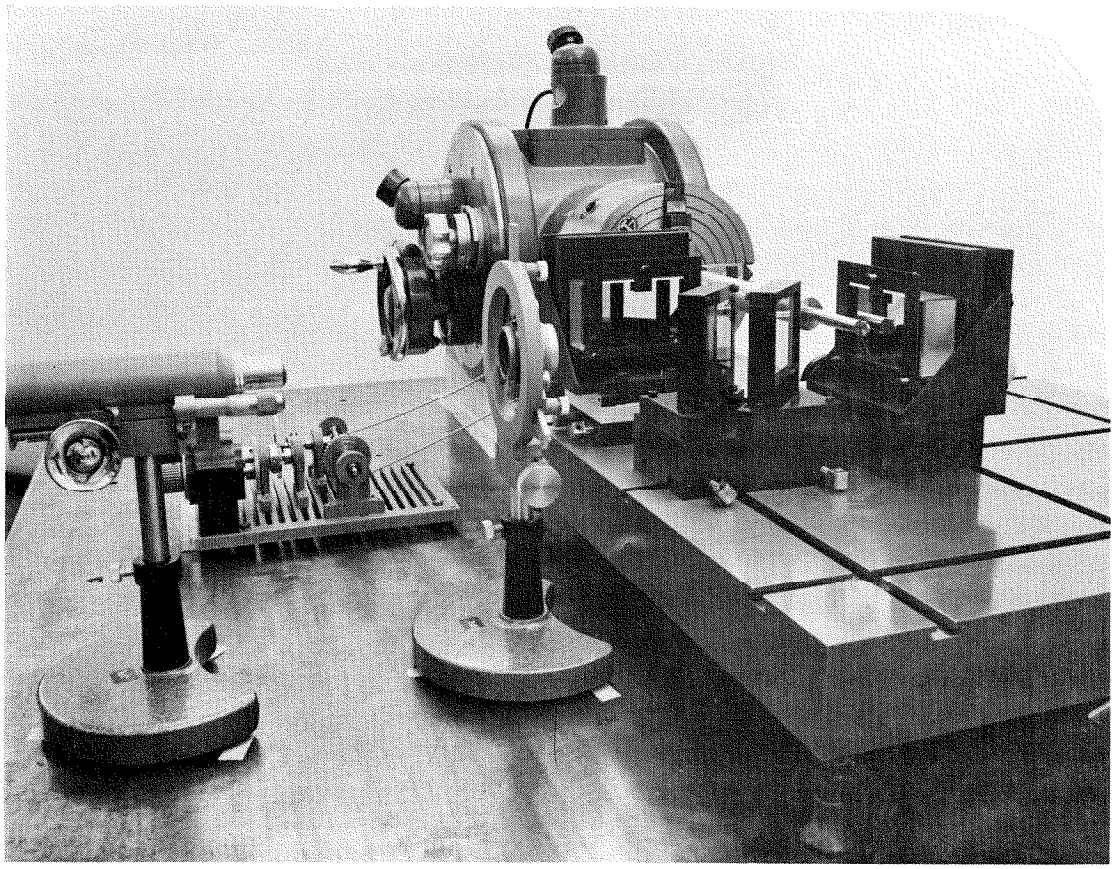

Figure 8: Photograph of the experimental apparatus showing the interferometer, the sample holder and the viewing optics.

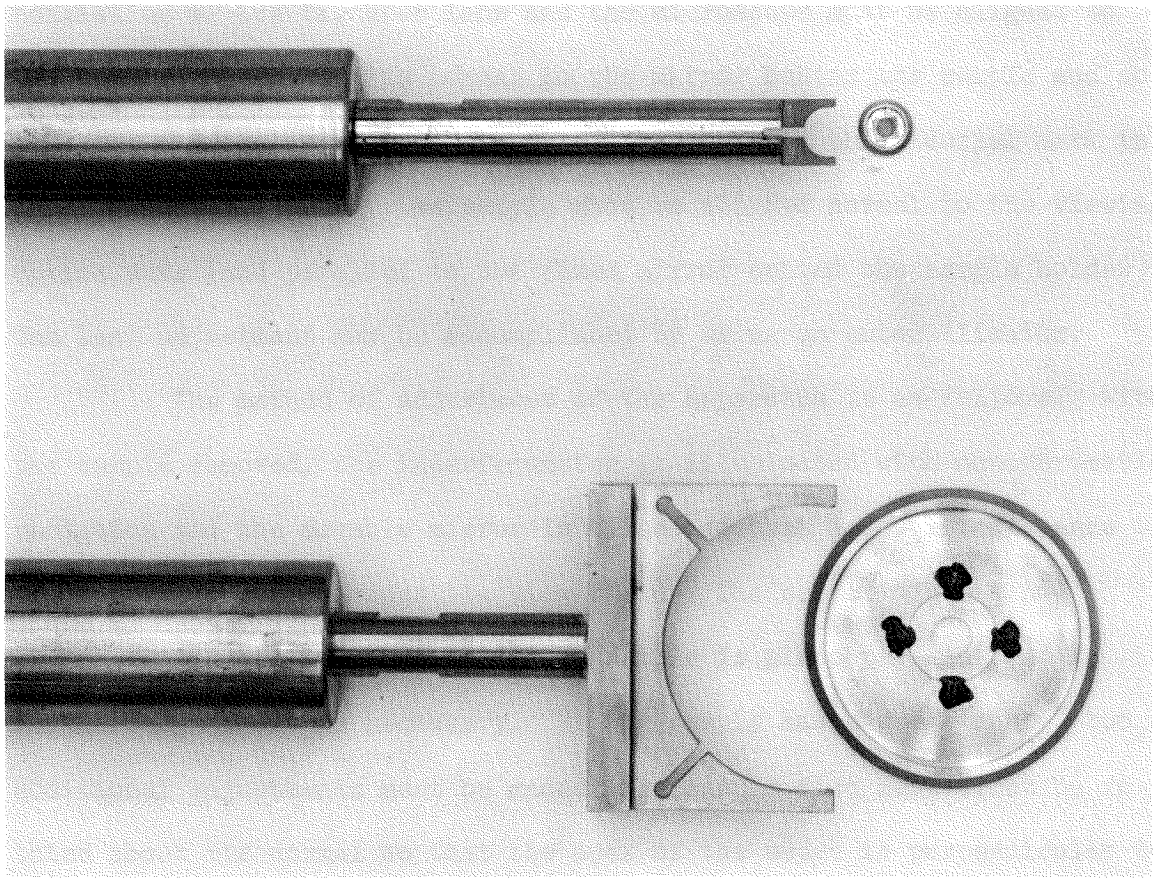

Figure 9: Photograph of the sample holders and discs.

must be as close as possible to the interferometer mirror and still allow free rotation of the sample holder. Second, the viewing optics consisting of the transfer lens and the microscope must be aligned so that their common axis is normal to the mirror behind the sample and so that the fiducial mark on the sample lines up with the fiducial mark in the microscope. Third, the sample must be aligned normal to the viewing optics axis (and parallel to the fixed mirror behind the sample holder). The last adjustment may be accomplished by using an autocollimator.

The method of adjustment of the apparatus is as follows. With the sample removed, the interferometer is illuminated with monochromatic radiation and the movable mirror is tilted so that a few interference fringes are visible across the view field. The sample disc is now placed in the sample holder. If the sample is plane parallel, no further adjustment is necessary. If the sample has a wedge angle, two additional adjustments must be made: the sample disc must first be rotated about its normal so that the apex of the wedge is perpendicular to the axis of rotation, and second, the mirror behind the sample must be adjusted so that the light beam returns on itself, as evidenced by the fringes viewed through the sample. Refocusing the microscope may be necessary to improve fringe visibility. For the case of a crystalline sample, the desired crystal axis must be aligned with the axis of rotation, and then the mirror behind the sample is adjusted so that the light beam returns on itself. In this case it may not be possible to have the apex of the wedge perpendicular to the axis of rotation.

4.2 Experimental Procedure

The apparatus described above may now be used to determine the refractive index and the slope of the refractive index.

1. Refractive Index

The interferometer is illuminated with monochromatic radiation of the desired wavelength, and the rotation angle is set to that for normal incidence. Normal incidence can be determined visually by finding the angle at which the fringe pattern remains stationary for small increments of the angle in either direction. The movable mirror is then translated so that a fringe is lined up with the fiducial mark in the viewing optics.

Fringe counting may then commence by slowly changing the rotation angle in one direction from normal incidence and noting the number of fringes passing the fiducial mark. It is convenient to stop the counting at some integral number of fringes, as previously discussed in Chapter II, however, a larger fringe count will give better accuracy.

It is sometimes experimentally difficult to determine the angle for normal incidence particularly if the sample is not plane parallel. In this case it is necessary to perform an additional measurement by counting fringes, while rotating the sample in the direction opposite to that used above through the same number of fringes counted above. The total angle between the two measured angles is twice the angle to be used in equation 2.10.

A separate determination of the sample thickness at the fiducial mark gives all the data necessary to use equation 2.10 to

calculate the refractive index.

2. Slope of the Refractive Index

The interferometer is illuminated with monochromatic radiation and the angle of the sample is set to that for normal incidence, and is not changed subsequently. The monochromatic source is then replaced with a continuously variable monochrometer whose input slit is illuminated with white light and whose output slit is placed at the focus of the collimating lens.

The sample is removed from the holder, and the movable mirror is positioned so that when the monochromator wavelength setting is changed, the observed fringe does not shift its position in the view field. The position of the mirror is then noted on the calibrated scale. The monochromator wavelength is then set to the desired wavelength and the sample is replaced in the holder. The movable mirror is translated so that the fringe at the sample fiducial mark does not shift position for small increments of the wavelength setting of the monochromator to either side of the desired wavelength. The change of the position of the movable mirror along with the refractive index and thickness of the sample gives all the data necessary to use equation 3.4 to calculate the slope of the refractive index.

In order to assure accuracy and repeatability of the above measuring techniques, each measurement should be repeated several times. It is quite difficult to attain repeatability in setting fringes to an accuracy of 1/100 of a fringe. Great care must be exercised in observing the fringe and the fiducial mark.

4.3 Use of a Visible Gas Laser as a Light Source

In one phase of the experiment at helium-neon CW gas laser operating at 6328Å was used as a monochromatic light source for the interferometer. Certain difficulties were encountered and are worthy of mention. The experimental setup is as shown in Figure 6 except that the lamphouse and collimating lens were replaced with the gas laser.

When the sample is viewed at normal incidence in monochromatic light from ordinary sources, the only fringe pattern visible is due to the light beam that traversed the sample to the mirror and back. The light beams that reflect from the sample faces generally do not cause fringe patterns because the optical path length difference for these beams exceeds the coherence length of the source (11). However, the coherence length of the radiation emanating from the gas laser is quite large, so that the sample reflected beams cause fringe patterns to appear.

As a result, three distinct fringe patterns are superimposed upon one another in the view field, one from the light beam reflecting from the mirror behind the sample, one from the back face of the sample and one from the front face of the sample. The only fringe pattern of interest is the one from the mirror, but the presence of the other two almost completely obscures the desired pattern, which makes it difficult to set a fringe to the reference mark on the sample. The unwanted fringe patterns disappear as soon as the sample is tipped away from normal incidence, so there is no problem in setting to a given fringe when $\theta \neq 0$.

The difficulties at normal incidence may be relieved somewhat if the interferometer is initially adjusted so that the desired fringe pattern is perpendicular to the axis of rotation of the sample. Then near normal incidence the undesired fringe patterns will be parallel to the axis of rotation, and will permit viewing the desired fringe pattern.

CHAPTER V

RESULTS

The apparatus described in the previous chapter was used to perform three distinct series of measurements. The first was an experimental verification of the accuracy and repeatability of the tipping method for refractive index determination, using samples whose refractive indices had already been determined by other methods. The apparatus was then used to determine the refractive indices of crystalline barium titanate. The last part was determination of the derivative of the refractive index $dn/d\lambda$ of barium titanate, as suggested in Chapter III. The determination of index gradients with temperature, voltage, etc., as outlined in Chapter III is an accepted method for the purpose, so no experimental verification was undertaken.

5.1 Accuracy and Repeatability

The verification of the accuracy and the repeatability of the tipping method for refractive index determination was accomplished by using the method to determine the refractive index of two different samples, flint glass and fused quartz, whose refractive indices had been previously determined by other methods. The test samples were made as plane parallel as feasible, and when viewed through the interferometer, appear to be within 1/5 wavelength of being flat (in transmission). The samples have a round shape, are approximately 12 mm in diameter, and are approximately 0.7 mm thick.

The flint glass sample was supplied by the manufacturer with

a set of measured refractive indices. The fused quartz sample was supplied with a prism that was fabricated from the same piece of material; the prism was made suitable for use on a Pulfrich refractometer, and was used on such a refractometer to measure the refractive index. The results of this measurement are reported in Appendix II.

In order to assure the highest possible accuracy, the interferometer was adjusted so that no more than three fringes were visible across the sample. Under this condition the repeatability in setting the angle was about 10 seconds in the worst case, which corresponds to an error in refractive index of 0.82×10^{-4}. The results of the measurements of the flint glass and the fused quartz samples are presented in Tables 3 and 4 respectively, using the thickness data presented in Appendix III.

The major cause of lack of repeatability at any given wavelength is an error in measurement of the change in interference order. In Section 2.2, it was shown that an error of 0.01 in interference order would produce an error in refractive index of 0.84×10^{-4}. The RMS deviation of the data points in Tables 3 and 4 compare favorably with this value.

The principal cause of a difference between the mean value of the measured refractive indices and the known refractive index is an error in measurement of the sample thickness. The maximum error is 1.2×10^{-4}, and is consistent with the theoretical error of 1.68×10^{-4} derived in Section 2.2. Thus, the agreement between the measured and known values for the Flint glass sample are within the

experimental error.

Inspection of Table 4 reveals that there is a difference of about 5×10^{-4} between the measured refractive indices and those determined by the Pulfrich refractometer. This difference is larger than the expected experimental error. The reason for this large error is due to the method used to measure the thickness of the quartz samples (see Appendix III). The comparison instrument used has enough pressure to cause 0.15μ depression of a steel gage block.[1] Since quartz has a modulus of elasticity that is 1/3 that of steel,[2] the comparison instrument will penetrate the quartz sample further than the steel gage block, producing an error in the indicated thickness of the quartz sample of approximately 0.3μ. This thickness error results in a calculated refractive index that is larger than the actual value. Corrected values for the refractive indices of the quartz standard are noted in Table 4. These values are within the expected experimental error of the Pulfrich refractometer values.

5.2 Determination of the Principal Indices of Refraction of Barium Titanate

It has been pointed out in Chapter I that there is a current need for determination of the refractive indices of barium titanate at as many wavelengths as possible. Present literature lists the principal indices of refraction of barium titanate as: $n_a = 2.42 \pm 0.036$,

---

1. Private communication from L. Brubaker, JPL Metrology Laboratory.

2. J. H. Perry, Chemical Engineers' Handbook, 3rd Edition McGraw-Hill, New York, 1950.

TABLE 3

REFRACTIVE INDEX OF FLINT GLASS STANDARD

Sample Thickness = 640.46μ

Wavelength	Fringe Count	Angle θ				Refractive Index n_s	
						Average and RMS Deviation	Previously Determined[3]
Å	m	deg	min	sec	Measured		
5460.74	50	18	56	21	1.62122		
	50	18	56	23	1.62116	1.62117 0.32×10^{-4}	1.62129
	100	26	33	15	1.62114		
5892.93	100	27	34	54	1.61847		
	100	27	35	0	1.61834	1.61841 0.65×10^{-4}	1.6185

3. Data supplied by manufacturer of glass

TABLE 4

REFRACTIVE INDEX OF FUSED QUARTZ STANDARD

Sample Thickness = 681.48μ

Wavelength	Fringe Count	Angle θ			Refractive Index n_s		
Å	m	deg	min	sec	Measured	Average and RMS Deviation	Previously Determined[4]
5460.74	50	20	10	0	1.46047		
	50	20	10	12	1.46023	1.46040^{5} 1.05×10^{-4}	1.45991
	100	28	10	36	1.46049		
	100	28	10	40	1.46043		
5892.93	50	20	57	9	1.45888		
	50	20	57	10	1.45886	1.45880^{6} 0.8×10^{-4}	1.45836
	100	29	15	5	1.45868		
	100	29	14	58	1.45878		

4. Measured by a Pulfrich Refractometer (see Appendix II).

5. Value corrected for error in thickness measurement: 1.46016

6. Value corrected for error in thickness measurement: 1.45849

$n_c = 2.347$ at 5460.74Å (15). The subscripts a and c refer to the crystal axis along which the $\vec{D}$ vector of the light is directed.

Barium titanate crystals are readily available from commercial suppliers,[7] but can be furnished only in the form of thin, flat plates which have moderately flat surfaces that consist of a series of plateaus and steps typical of the face of a grown crystal. The surfaces are in general not parallel to each other, however, the wedge angle between them is usually only a few minutes of arc. At room temperature barium titanate has a tetragonal crystal structure and is optically uniaxial. The optical axis is usually normal to the plane of the crystal plates, but it is possible to obtain a crystal with the optic axis in the plane of the plate by a proper annealing process. The crystal plates of barium titanate are extremely brittle and fragile, and it is not practical to polish the surfaces to remove the steps in order to improve the optical quality of the plates.

The optical quality of the crystal plates is good enough so that fringes are visible when the plate is viewed through a Twyman-Green interferometer. The effect of the steps in the crystal faces is to produce indistinct fringes that move in discrete jumps as the sample is rotated away from normal incidence.

Two samples of barium titanate were prepared for use in the refractive index determination. Each sample was approximately 3 mm square and 0.2 mm thick, and was mounted upon a brass disc which had a

---

7. Harshaw Scientific Company is one such source of supply.

2.5 mm hole through it. The samples are identified by the numbers 80 and 84. Sample No. 80 was annealed so that the optic axis lay in the plane of the sample, and sample No. 84 was prepared so that its optic axis was normal to the plane of the sample. Sample No. 80 had a 5.8 minute wedge angle and sample No. 84 had an 8.6 minute wedge angle. Sample No. 84 was of better optical quality than sample No. 80, the latter having many noticeable steps across its face. When the samples were placed in the interferometer, it was not possible to obtain less than 10 or 12 fringes across the aperture of the sample because the samples were slightly convex, and the fringe pattern became too distorted if an attempt was made to attain less fringes. It was not possible to orient the apex of the wedge angle of Sample No. 80 perpendicular to the axis of rotation of the dividing head, since it lay at an angle of approximately 30° to the $\bar{a}$ crystal axis. Sample No. 84 was oriented with the apex perpendicular to the rotation axis, however.

Seven wavelengths in the visible portion of the spectrum were used to determine the refractive indices. The wavelengths used and their sources are listed as follows:

4358.35	Mercury Discharge Lamp
5460.74	
5790.65	
5085.82	Cadmium Discharge Lamp
5350.46	Thallium Discharge Lamp
5892.93	Sodium Discharge Lamp
6328.17	Helium-Neon Gas Laser

The results of the refractive index determination of barium titanate using the tipping method are presented in Tables 5 and 6, using thickness data presented in Appendix III. Sample No. 80 was used to measure both n_a and n_c since its optic axis is in the sample plane, and the results are presented in Table 5. Sample No. 84 was used to measure n_a only and the results appear in Table 6. The data for n_c appearing in Table 6 was obtained by using the values listed for $n_a - n_c$ in reference (16) given that at 5460.74Å, $n_a - n_c = .073$ (15).

Inspection of Figure 10 shows that there is an apparent difference in the refractive indices of the two samples. This could be partly due to errors in measuring the crystal thicknesses. Meyerhofer (17) points out however, that there is an unexplained difference in refractive index between samples of barium titanate, which could be given as the reason for the slightly different shape of the curves for the two samples in the 5000-6000Å region.

The value for refractive index obtained for sample No. 84 at 4358Å appears to be low. This may be explained by the fact that barium titanate has an absorption edge near 4000Å, which would cause the refractive index to decrease as the absorption coefficient increases. Hornig (18) reports experimental evidence about induced birefringence in barium titanate which substantiates this contention.

These results may now be used to estimate whether or not the "velocity matching" discussed in Chapter I is possible. In order for velocity matching to be possible, the value of n_a at the fundamental wavelength must be greater than the value of n_c at the second harmonic

TABLE 5

PRINCIPAL REFRACTIVE INDICES OF BARIUM TITANATE

Sample No. 80 Thickness = 179.1μ Temp. = 25°C

1. $\vec{D}$ vector along $\vec{a}$ axis.

Wavelength Å	Fringe Count m	Angle θ deg	min	sec	Refractive Index n_a
5085.82	50	27	48	3	2.4700
	100	39	7	44	2.4609
5350.46	50	28	36	45	2.4410
	100	40	11	31	2.4440
5460.74	50	28	55	2	2.4369
	50	28	55	30	2.4348
	100	40	40	7	2.4288
	100	40	39	47	2.4300
5790.65	50	29	50	43	2.4166
	100	41	54	11	2.4180
5892.93	50	30	8	36	2.4068
	100	42	19	29	2.4059
6328.17	50	31	17	45	2.3885
	100	43	56	11	2.3836

TABLE 5 - Cont.

2. D vector along $\bar{c}$ axis.

Wavelength Å	Fringe Count m	Angle θ deg	min	sec	Refractive Index n_c
5085.82	50	28	5	12	2.3929
	100	39	28	41	2.3891
5350.46	50	28	52	12	2.3749
	100	40	33	45	2.3706
5460.74	50	29	11	43	2.3667
	100	41	0	3	2.3643
5790.65	50	30	5	45	2.3560
	100	42	15	27	2.3513
5892.93	50	30	24	14	2.3450
	100	42	40	47	2.3403

TABLE 6

PRINCIPAL REFRACTIVE INDICES OF BARIUM TITANATE

Sample No. 84 Thickness = 226.24μ Temp. = 25°C

Wavelength Å	Fringe Count m	Angle θ deg	min	sec	Refractive Index n_a	n_c [8]
4358.35	25	16	14	11	2.4813	2.374
	50	22	54	32	2.4821	
5085.82	50	24	46	47	2.4663	2.386
	100	34	52	13	2.4673	
5350.46	50	25	29	16	2.4429	2.368
	100	35	51	0	2.4443	
5460.74	50	25	45	38	2.4387	
	50	25	46	10	2.4361	
	50	25	45	38	2.4387	2.365
	100	36	14	13	2.4384	
	100	36	14	35	2.4371	
5790.65	50	26	34	45	2.4216	
	50	26	34	46	2.4215	2.354
	100	37	22	47	2.4198	
5892.93	50	26	50	19	2.4137	2.347
	100	37	43	44	2.4139	

8. Calculated from n_a using birefringence data from Reference 16.

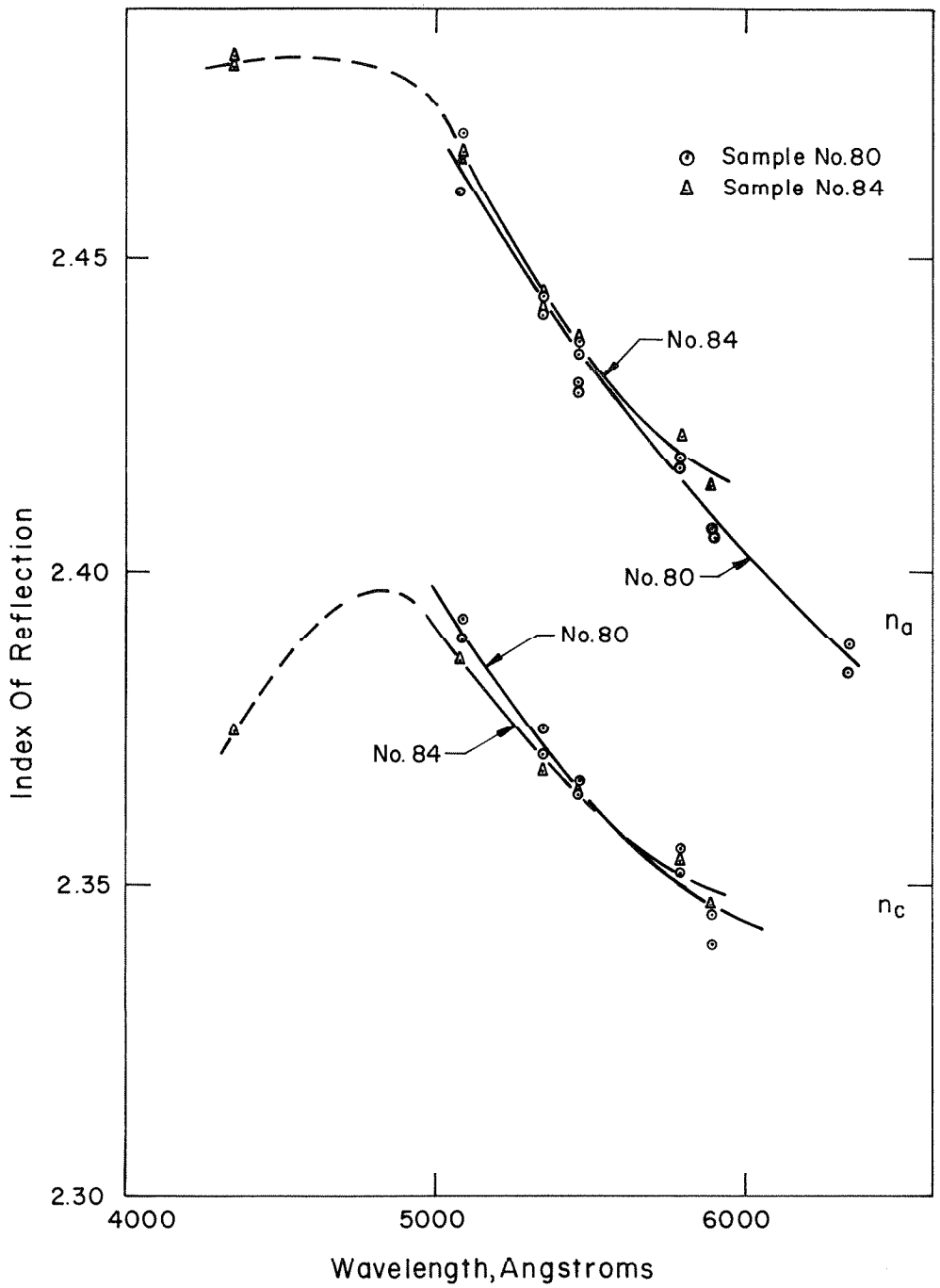

Figure 10: Principal indices of refraction of barium titanate at a temperature of 25°C.

wavelength. Visual extrapolation of the curves of Figure 10 out to 10,000Å seems to indicate that the above condition cannot be fulfilled.

5.3 Derivative of the Refractive Index of Barium Titanate

In order to obtain refractive index data for barium titanate over a wider wavelength range than that used for the data reported above, the slope of the refractive index of sample No. 84 was determined using the method presented in Chapter III.

The sample was removed from the interferometer and the movable mirror was positioned so that white light fringes were visible and the central (zero order) fringe registered with the fiducial mark. The sample was then replaced on the interferometer and the interferometer was illuminated with the monochromator as described in Chapter IV. With the monochromator set to a given wavelength, the movable mirror was positioned so that the fringe coincident with the fiducial mark remained stationary when the wavelength setting was changed slightly in either direction. Table 7 presents the results of these measurements.

Using equations 3.4 and 3.5 and the data from Tables 6 and 7, Table 8 may be constructed. The values for the refractive index appearing in Table 8 were obtained as follows: 4610Å - 5085Å, use of equations 3.4 and 3.5 backwards from 5085Å; 5085Å - 5893Å, average value of refractive indices appearing in Table 6; 5893Å - 6800Å, use of equations 3.4 and 3.5 forwards from 5893Å.

The accuracy of the extrapolated results presented in Table 8 is not too high, and is intended only to show the general dependence of the refractive index upon wavelength. It is interesting to note that

TABLE 7

DATA FOR REFRACTIVE INDEX DERIVATIVES OF BARIUM TITANATE SAMPLE NO. 84

Mirror Position for no sample: 17.080

Wavelength Å	Mirror Position
4610	17.598
4800	17.561
5000	17.540
5085	17.531
5350	17.507
5461	17.499
5790	17.487
5893	17.471
6000	17.468
6200	17.460
6330	17.455
6800	17.442

TABLE 8

REFRACTIVE INDEX AND DERIVATIVE OF REFRACTIVE INDEX OF BARIUM TITANATE

Sample No. 84 Thickness = 226.24μ Temp. = 25°C

Wavelength Å	Refractive Index		Derivative of Refractive Index
	Measured	Computed[9]	$dn/d\lambda$, μ^{-1}
4610	-	2.523	-1.663
4800	-	2.498	-1.309
5000	-	2.476	-1.115
5085	2.4668	-	-1.037
5350	2.4435	-	-0.830
5461	2.4385	-	-0.749
5790	2.4216	-	-0.583
5893	2.4138	-	-0.534
6000	-	2.408	-0.512
6200	-	2.398	-0.454
6330	-	2.392	-0.420
6800	-	2.372	-0.335

9. Computed using data for $dn/d\lambda$ and equation 3.5.

there is no indication of a decrease in value of the derivative of the refractive index below 5000Å, as the results of the previous section had indicated. Further research will be necessary to resolve this question.

CHAPTER VI

CONCLUSIONS

The problem of determination of the index of refraction of a thin, flat plate of optical material has been considered. Two methods are discussed, both of which are based upon determination of the optical path length through the sample using an interferometer. The first method is based upon direct determination of the path length, but is shown to be limited in the type of samples it will accommodate. In the second method the path length is determined indirectly by tipping the sample away from normal incidence. This method is shown to be quite versatile in the class of samples it can use. In addition to determination of index of refraction, methods for determination of gradients of refractive index with temperature, electric field, magnetic field, etc., and wavelength of the illuminating radiation are considered.

An apparatus for index of refraction determination based upon the tipping method has been constructed using a Twyman-Green interferometer. An error analysis is presented which shows that the apparatus has an ultimate accuracy of $\pm 2 \times 10^{-4}$ in refractive index. This accuracy is experimentally verified by measurement of the refractive indices of two samples whose refractive indices have been previously determined by other methods.

The tipping method is then applied to the measurement of the principal refractive indices of single crystal barium titanate at several wavelengths in the visible spectrum. Barium titanate is a

material that is currently of interest because of its ability to generate second harmonic radiation of laser light. The results of the refractive index determination of barium titanate indicate that the "velocity match" condition for harmonic generation probably cannot be met. The accuracy of the results for barium titanate is not good due to the poor optical quality of the samples used. These results could be improved by using a thicker sample of barium titanate that has polished faces to improve its optical quality.

The tipping method of refractive index determination has moderate accuracy and good applications to materials that can be obtained only in thin, flat plates. The quantity and type of apparatus necessary for the method is such that it is not practical as a general method for refractive index determination. The apparatus is currently limited to use in the visible portion of the spectrum; however, the addition of a photoelectric fringe counting device would extend the range of the apparatus to the ultraviolet and the near infrared.

APPENDIX I

DESCRIPTION OF A SHOCK MOUNT FOR A SURFACE PLATE

The interferometer used in the experimental apparatus described in Chapter IV is sensitive to vibration. In order to have the ability to set a fringe pattern to a fiducial mark repeatably to within 0.01 fringe, it is necessary to isolate all possible vibration from the interferometer. With the interferometer placed upon a 1000 pound steel surface plate, the building vibration was still sufficient to produce a random shift in the fringe pattern that had an approximate magnitude of 0.5 of a fringe peak-to-peak.

It was thus necessary to construct a shock mounting device for the apparatus. In order to provide the maximum amount of isolation, the shock mount was built to carry the entire surface plate upon which the apparatus was placed. The active portion of the shock mount consists of four 5.70 x 8 industrial inner tubes all connected to a common inflation manifold. The inner tubes are symmetrically placed between two 3' x 4' pieces of 3/4" thick plywood, and the entire assembly is then located between the surface plate support frame and the bottom of the surface plate. Small 2" high spacer blocks are placed at the corners of assembly between the two pieces of plywood to prevent the weight of the surface plate from crushing the inner tubes when they are deflated. Figure 11 is a drawing of the shock mount assembly.

The use of the shock mount is quite simple. The inner tubes are inflated through the common inflation manifold with enough air to

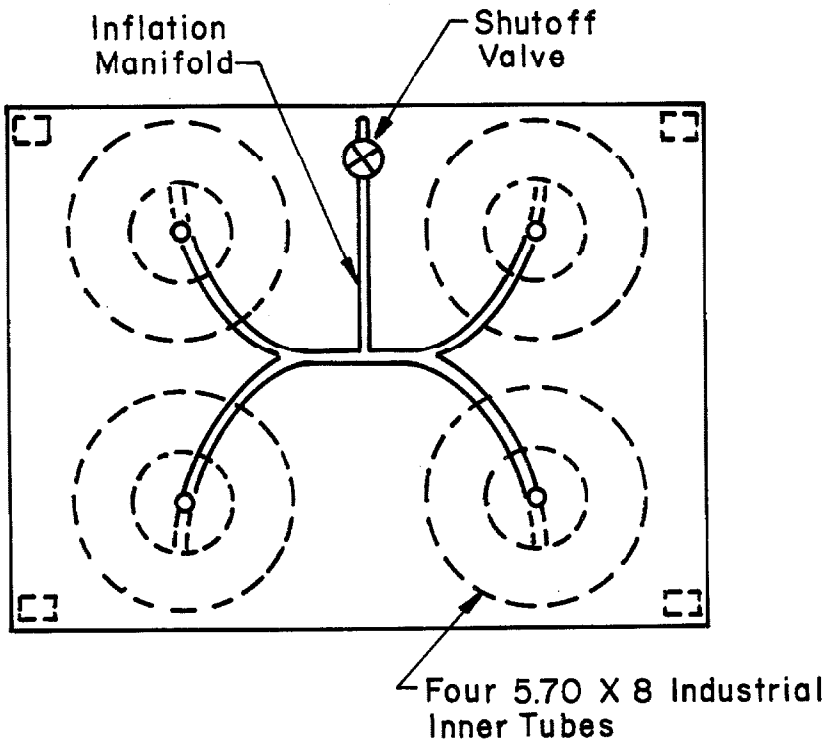

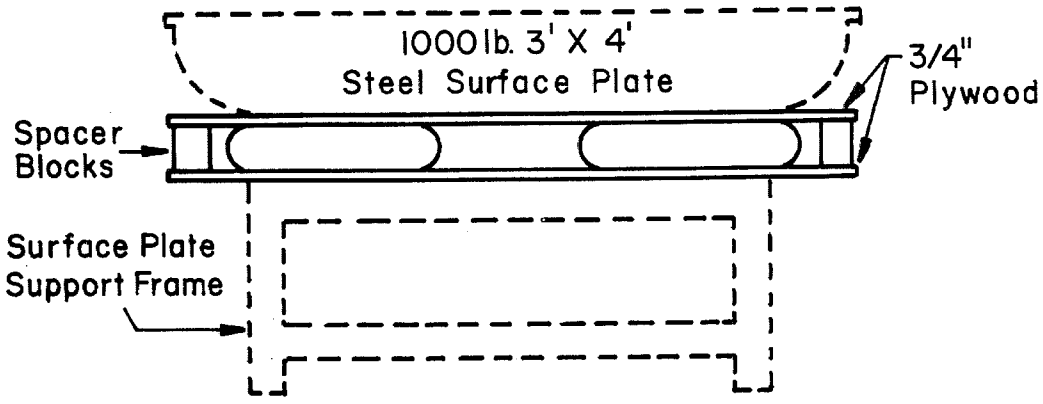

Figure 11: Drawing of the shock mount for the table used to support the experimental apparatus.

raise the top piece of plywood 1/2" off the spacer blocks. The pressure in the inner tubes required to do this is approximately 2.5 p.s.i. Due to an uneven mass distribution of the apparatus on the surface plate, the surface plate may not be level. It is then necessary to deflate the inner tubes and shift their position slightly to correct for this condition.

The effect of the installation of the above shock mount upon the random shift in the fringe pattern of the interferometer was to reduce it to less than the instrument resolution, 0.01 fringe.

APPENDIX II

MEASUREMENT OF THE REFRACTIVE INDEX OF A QUARTZ PRISM

The measurement of the refractive index of the quartz used as a standard for this research was accomplished by the method described below. From the same quartz ingot used to make the flat plates for the measurement reported in Section 5.1, two 90° prisms were constructed. The refractive index of these prisms was then measured on a commercial Pulfrich refractometer. Tilton and Taylor (9) describe the method in detail.

The results of the measurement are presented in the following table. Each data point was checked four times to insure repeatability.

TABLE 9

REFRACTIVE INDEX OF QUARTZ PRISMS

	Prism No. 1		Prism No. 2	
Wavelength	Angle	Refractive Index	Angle	Refractive Index
5460.74	45° 9'	1.45991	45° 9'	1.45991
5892.93	44° 38'	1.45836	44° 38'	1.45836

APPENDIX III

MEASUREMENT OF THE THICKNESS OF THE SAMPLES

The thickness of all samples used for this research were measured by the gage block comparison technique with some minor variations as described below. The stated accuracy of this method is ± 0.05 microns.

The thickness of the quartz sample was measured using a comparison instrument that contacted the sample on each side with .1250" radius diamond balls using 110 gm. pressure. The comparison standard was a steel gage block with known thickness.

The thickness of the flint glass sample and the barium titanate samples were measured using a comparison instrument that contacted the sample on one side with a 0.1250" diameter steel ball using 4 gm. pressure. The other side of the sample was placed upon a reference flat. As above, the comparison standard was a steel gage block. Proper corrections in the thickness measured were made to account for the air film between the sample and the reference flat.

The results of the thickness measurements are presented in the following table.

TABLE 10

SAMPLE THICKNESS

Sample	Thickness, microns
Quartz	681.48
Flint Glass	640.46
Barium titanate sample No. 80	179.1
Barium titanate sample No. 84	226.24

REFERENCES

1. P. A. Franken, A. E. Hill, C. W. Peters and G. Weinreich, Phys. Rev. Letters 7, 118 (1961).

2. J. A. Giordmaine, Phys. Rev. Letters 8, 19 (1962).

3. P. D. Maker, R. W. Terhune, M. Nisenoff and C. M. Savage, Phys. Rev. Letters 8, 21 (1962).

4. J. A. Armstrong, N. Bloembergen, J. Ducuing and P. S. Pershan, Phys. Rev. 127, 1918 (1962).

5. P. A. Franken and J. F. Ward, Rev. Modern Physics 35, 23 (1963).

6. D. A. Kleinman, Phys. Rev. 128, 1761 (1962).

7. A. Savage and R. C. Miller, Appl. Optics 1, 661 (1962).

8. R. C. Miller, D. A. Kleinman and A. Savage, Phys. Rev. Letters 11, 146 (1963).

9. L. W. Tilton and J. K. Taylor, "Refractive Index Measurement", Physical Methods in Chemical Analysis, Vol. I, 2nd Ed., Academic Press, New York, pp. 411-462.

10. C. A. Proctor, Phys. Rev. 24, 195 (1907).

11. M. Born and E. Wolf, Principles of Optics, Pergamon Press, New York, 1959.

12. S. Tolansky, An Introduction to Interferometry, Longmans, Green and Co. London, 1955.

13. G. N. Ramachandran and S. Ramaseshan, "Crystal Optics", Handbuch Der Physik, Vol. XXV/1, Springer-Verlag, Berlin, 1961.

14. W. E. Williams, private communication.

15. F. Jona and G. Shirane, Ferroelectric Crystals, MacMillan Co. New York, 1962.

16. L. E. Cross, M. M. Nicholson, B. Zlotnicki and R. Whiddington, Nature 165, 440 (1950).

17. D. Meyerhofer, Phys. Rev. 112, 413 (1958).

18. A. W. Hornig, "Electro-optics and Paramagnetic Resonances in Barium Titanate Single Crystals", Ph.D. Dissertation, Stanford University (1955).